

DEVELOPMENT OF VIRTUAL NATURAL LIGHTING SOLUTIONS WITH A SIMPLIFIED VIEW USING LIGHTING SIMULATION

R.A. Mangkuto, M.B.C. Aries, E.J. van Loenen, and J.L.M. Hensen
Unit Building Physics and Services, Department of the Built Environment
Eindhoven University of Technology, Eindhoven, the Netherlands

ABSTRACT

Computational building performance simulation can be employed to develop various future solutions. The development of Virtual Natural Lighting Solutions (VNLS), which are systems that artificially provide natural lighting and view comparable to those of real windows and skylights, is steered by modelling them as arrays of small light sources resembling a simplified view of a blue sky and green ground. The lighting simulation tool *Radiance* is employed to predict the space availability, uniformity, ground light contribution on the ceiling, and probability of discomfort glare. The input variables are “distance between windows”, “tilt angles”, “beam angles”, and “total luminous fluxes of the sky elements”. Sensitivity analysis shows that the total luminous flux positively influences the space availability, the beam angle positively influences the uniformity; and negatively influences average ground light contribution on the ceiling and average probability of discomfort glare. Most of the VNLS models with 114° beam angle perform better on the tested performance indicators than real windows under CIE overcast sky.

INTRODUCTION

Many researchers have shown that health and wellbeing of people is strongly influenced by the presence of daylight. Several studies have reported that people with sufficient access to daylight experience less stress, have a higher productivity, and are more alert (e.g., Heschong et al., 2002; Heschong, 2003; Boyce, 2003). However, daylight is largely variable and is limited in time and space.

In situations where daylight is not or insufficiently available, the Virtual Natural Lighting Solution (VNLS) concept can be promising. VNLS are systems that can artificially provide lighting and an outside view, with properties comparable to those of real windows and skylights. The benefit of installing VNLS in a building is the ability to use more space which has very limited or no access to daylight, with the possibility of controlling the lighting and view quality (Mangkuto et al., 2011).

Currently, there is very little discussion about the implication of applying such a system with regard to

building performance, which can be described in terms of its lighting quality and energy consumption. Since VNLS are future systems with many possible input variables, it is reasonable to employ computational building performance simulation for predicting their performance (Mangkuto et al., 2012a). We applied *Radiance* (Ward and Shakespeare, 1998) as the main tool for lighting simulation, in which the VNLS were modelled as arrays of small light sources with a simplified view of the ground and the sky.

The work in this paper focuses only on the numerical design appraisal of the ongoing development of VNLS, while physical models are not yet realised. As a contribution to steer the development process of such a future solution, this study is meant to demonstrate the role of building performance simulation in the development process of VNLS, by predicting the performance of a numerical model of VNLS relative to that of real windows. The work has two objectives:

1. To understand the effect of varying input variables of the VNLS model on the lighting performance of the given space.
2. To compare the lighting performance of the simulated VNLS in the given space, relative to that of simulated real windows under the CIE overcast sky.

The lighting performance indicators in this study are the space availability (percentage of workplane meeting a certain minimum illuminance value), the illuminance uniformity on the workplane, the illuminance contribution from the “ground” elements on the ceiling, and the probability of discomfort glare at observer positions. A VNLS ideally provides space availability comparable to or better than real windows with the same configuration and equal or less glare perception.

METHOD

Basic principle

According to the split-flux method for real windows under the CIE overcast sky (Tregenza, 1989), the daylight component in general can be split into three parts, i.e. sky, externally reflected, and internally reflected components. The sky component (SC)

represents direct light from the patch of sky visible at the point considered. The externally reflected component (ERC) comes from opposing exterior surfaces, while the internally reflected component (IRC) enters through the window and reaches the point after reflection from interior surfaces. From the illustration in Figure 1, it is seen that the internally reflected component partly comes from the exterior ground reflection.

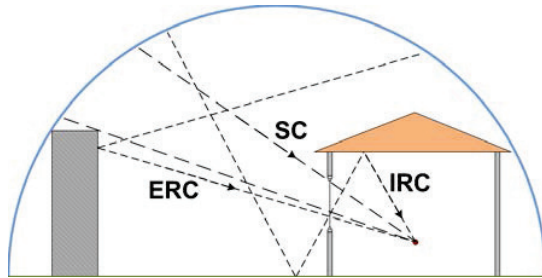


Figure 1 Schematic illustration of the three daylight components

In this study, we modelled the VNLS as arrays of small light emitting areas, displaying an image scene of a simplified green ground (horizon) and blue sky. As there are no exterior objects in the view, the externally reflected component is absent. The internally reflected component is partly provided by the bottom array, which acts as the “ground”, tilted upward and direct the light to the ceiling. The rest of the light sources act as the “sky”, tilted downward to deliver the light to the workplane area, providing the sky component as illustrated in Figure 2.

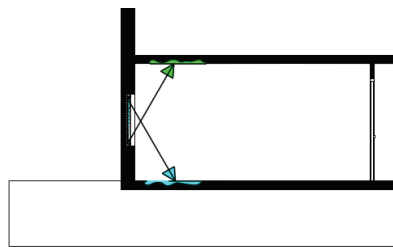


Figure 2 Schematic illustration of the VNLS with a simplified view and directional light

Model description

Two light emitting areas were modelled to fit two individual vertical windows, each with the size of $0.80 \text{ m} \times 1.21 \text{ m}$ ($W \times H$), corresponding to a window-to-wall ratio of 20%. At the lowest row in each individual window, there are four light emitting source areas ($0.20 \text{ m} \times 0.20 \text{ m}$ each) resembling a green “ground” surface. On top of them, there are 20 rows of “sky” sources with individual size of $0.05 \text{ m} \times 0.05 \text{ m}$, resembling a blue sky.

Four input variables were introduced in the model to understand the effect of changing the input variables

to the relevant performance indicators. The input variables are as follows:

1. *Interval of tilt angle.* To model the directionality of the incoming light, the “sky” sources were tilted downward with a certain interval of tilt angle. The sources at the row directly above the “ground” are at all times not tilted (i.e. 0°), while the sources at the second row above the “ground” were tilted downward by 1.0° , or 1.5° , or 2.0° . The sources at the third row above the “ground” were tilted downward by 2.0° , or 3.0° , or 6.0° , and so on. As a result of using the defined window height, the sources at the top row were tilted downward by 20° , 30° , or 40° . The “ground” sources were tilted with a 40° angle pointing upward.

Figure 3 displays the views of an individual VNLS with upper tilt angle of 40° .

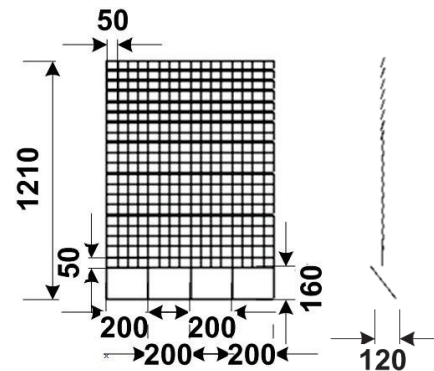
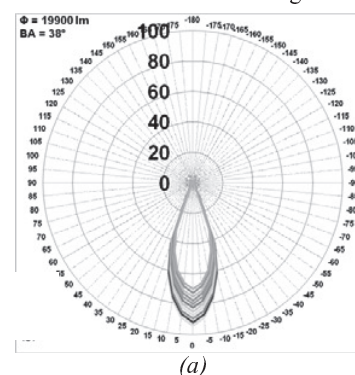


Figure 3 Front and side views of the modelled individual VNLS with simple view and directional light, with an upper tilt angle of 40°

2. *Beam angle.* The sources have a certain beam angle, i.e. the angle between the two directions opposed to each other over the beam axis for which the luminous intensity is half that of the maximum luminous intensity. To see the effects of varying beam angle, three values of beam angle for the “sky” were used, i.e. 38° (relatively narrow spread), 76° (medium), and 114° (wide, nearly diffuse). Figure 4 illustrates three examples of the luminous intensity polar diagram of the “sky” sources with each beam angle.



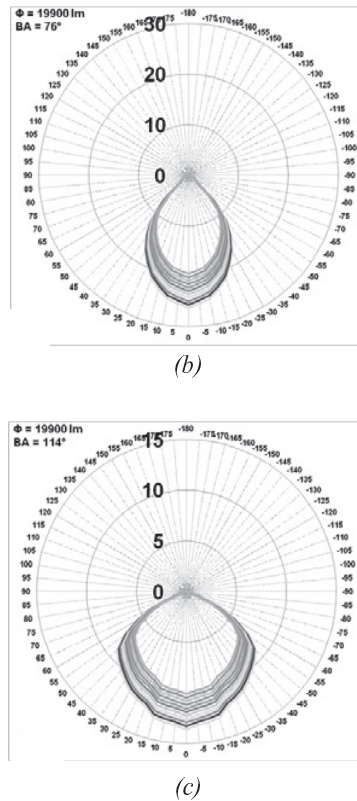


Figure 4 Examples of polar diagram of luminous intensity (in candela) of the light sources resembling the sky, with beam angle of (a) 38° , (b) 76° , and (c) 114°

Each “ground” source has a maximum intensity of 110 cd at the low luminance setting, 199 cd at the medium one, and 354 cd at the high one; all have a similar pattern of luminous intensity distribution. A tilt angle of 40° upward was chosen so that the “ground” sources do not stand completely vertical, which can possibly create too much glare; and that they are not tilted too much, which can reduce the visibility of the “ground” itself.

3. *Total luminous flux.* The total luminous fluxes of all “sky” sources (two individual windows) were set to be approximately 6200 lm, 11100 lm, and 19900 lm, representing the low, medium, and high luminance settings. For the “sky” sources with a 114° beam angle (nearly diffuse), these values correspond to an average surface luminance of 1000 cd/m^2 , 1800 cd/m^2 , or 3200 cd/m^2 ; which are the first three values used in the experiments of Shin et al. (2012). The intensity values for the “sky” sources with 38° and 76° beam angles were adjusted accordingly, so that the total luminous flux coming from the “sky” sources altogether remains the same.

4. *Distance between individual windows.* Two window configurations were used; the first one has no space between the two individual windows, while the other has a distance of 0.75 m. The simulated space has the size of a reference office room (van Dijk and Platzer, 2003), i.e. $5.4 \text{ m} \times 3.6 \text{ m} \times 2.7 \text{ m}$ ($L \times W \times H$), with windows only in the façade, as illustrated in Figure 5.

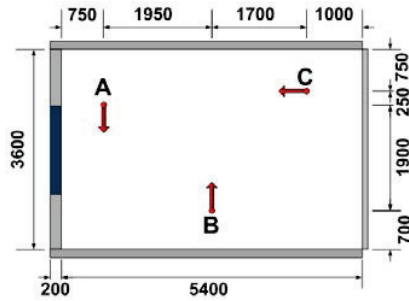


Figure 5 Plan view of the simulated reference office space

These window configurations were taken from the earlier studies of Diepens et al. (2000) and Lawrence Berkeley National Laboratory (LBL) (2010), as illustrated in Figure 6.

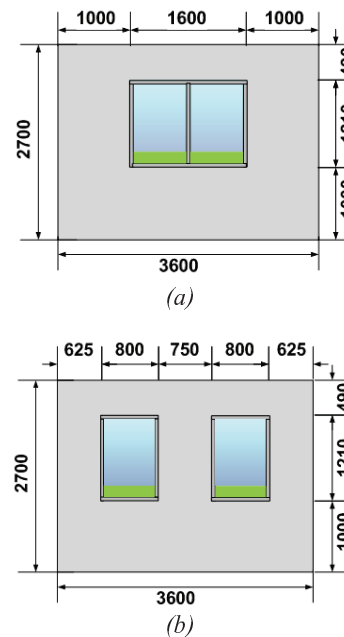


Figure 6 Elevation view of the VNLS window configuration on the wall, with a distance between individual windows of (a) 0 and (b) 0.75 m

Simulation settings

Simulations were run individually for every variation of the VNLS. The ambient parameters used in *Radiance* were set as displayed in Table 1.

Table 1
Radiance ambient parameters used in the simulations

Parameter	Description	Value
-ab	Ambient bounces	4
-aa	Ambient accuracy	0.08
-ar	Ambient resolution	128
-ad	Ambient divisions	1024
-as	Ambient super-samples	256

Evalglare (Wienold and Christoffersen, 2006) was employed to calculate glare indices for three different observer positions (see Figure 5), namely A, B, and C, defined at the eye height of 1.2 m above the floor. Position A is near the window and viewing parallel to the window plane, B is in the middle of the room and viewing parallel to the window plane opposite to the viewing position A, while C is near the rear wall and directly facing the window plane.

Assessment

The assessment was performed to evaluate the performance indicators of interest, which are:

1. *Space availability* (%A), that is the percentage of workplane area at height of 0.75 m with illuminance equal to or larger than 500 lx, i.e. the typical value for office work (CEN, 2002). It can be expressed as follows:

$$\%A = \frac{n(E \geq 500 \text{ lx})}{N} \times 100\% \quad (1)$$

where $n(E \geq 500 \text{ lx})$ is the number of points with illuminance $\geq 500 \text{ lx}$, and N is the total number of points. In this case, $N = 54 \times 36 = 1944$ points.

2. *Uniformity* (U_0), that is the ratio between the minimum illuminance (E_{\min} [lx]) to the average (E_{av} [lx]), based on the defined calculation points.

$$U_0 = \frac{E_{\min}}{E_{av}} \quad (2)$$

3. *Ground contribution* (%G), that is the percentage ratio of illuminance contribution from the "ground" element sources (E_{ground} [lx]), to the total illuminance received at a certain point on the ceiling (E_{total} [lx]), with the surface normal facing downward (z-axis); as expressed in Equation 3. There are 10 points ($N = 10$) defined in a line on the ceiling. The average value is then reported as $\%G_{av}$, expressed in Equation 4.

$$\%G = \frac{E_{\text{ground}}}{E_{\text{total}}} \times 100\% \quad (3)$$

$$\%G_{av} = \frac{\sum_{i=1}^N \%G_i}{N} \quad (4)$$

4. *Average probability of discomfort glare* (PDG_{av}), that is the average of the normalised values of all potentially relevant glare indices, i.e. Daylight Glare Probability (DGP), Daylight Glare Index (DGI), Unified Glare Rating (UGR), and CIE Glare Index (CGI). The normalisation procedure is according to Jakubiec and Reinhart (2012), i.e.:

$$DGI_n = 0.01452 \times DGI \quad (5)$$

$$UGR_n = 0.01607 \times UGR \quad (6)$$

$$CGI_n = 0.01607 \times CGI \quad (7)$$

Hence:

$$PDG_{av} = (DGP + DGI_n + UGR_n + CGI_n)/4 \quad (8)$$

In turn, to evaluate the influencing effect of the current input variables on the defined performance indicators, sensitivity analysis using multiple linear regressions was performed. The problem was then solved in MATLAB to determine the standard regression coefficients (β') that determine the sensitivity of the output as function of the input.

As a means of comparison, the VNLS in all configurations were replaced with real windows (double clear glass 6 mm, transmittance 88.5%) under a CIE overcast sky condition. This comparison is necessary, since the display of a simplified image of blue sky and green ground is an important feature of the proposed VNLS model, which should also be compared with a relatively simple view of overcast sky and plain ground outside the real windows. Moreover, this VNLS type is designed to increase the possibility of perceiving the direct light components from the sky and reflected light components from the ground, on the interior surfaces. This impression often appears in a space with real windows.

The sky condition of the real windows scenes was modelled in *Radiance* by defining the zenith brightness value [$W/(sr \cdot m^2)$], chosen in a way so that the interior surface of the window will give approximately the same average luminance as the corresponding VNLS. Note that VNLS with the same total luminous flux can have a different average surface luminance, particularly when the beam angles are different. Therefore, each VNLS scene was compared only to the real window scene with approximately the same average surface luminance.

For example, VNLS with $\Phi = 11100 \text{ lm}$ and $BA = 114^\circ$ has an average surface luminance of 1800 cd/m^2 , while VNLS with $\Phi = 11100 \text{ lm}$ and $BA = 76^\circ$ has 3200 cd/m^2 . These values correspond to a zenith brightness of 39 and 69 $W/(sr \cdot m^2)$, or

approximately 17000 and 30000 lx of exterior illuminance under the CIE overcast sky.

To evaluate the performance of all VNLS variations, four performance criteria were applied on the relative comparison between performance indicators of the VNLS and the real windows with the same average surface luminance. These were based on the expected benefit of having VNLS, i.e. gaining more well-lit and uniform space; while maintaining the ground contribution on the ceiling and the probability of discomfort glare comparable to those in real windows scenes. We defined the criteria in terms of a ratio, evaluated up to one significant digit after the decimal point. The criteria are:

- The VNLS should create larger space availability, compared to the real windows.
- The VNLS should create equal or better illuminance uniformity, compared to the real windows.
- The VNLS should create average ground contribution on the ceiling that is within $\pm 10\%$ of that in the real windows scene.
- The VNLS should create equal or smaller average probability of discomfort glare as observed in position C, compared to the real windows.
- The VNLS should have an average surface luminance of not larger than 3200 cd/m^2 , which is the value given in the experiments of Shin et al. (2012), where the subjects on average perceived the glare from the virtual windows as “acceptable”, i.e. got a score of 2.5 out of 4.5 on their discomfort glare scale.

RESULTS AND DISCUSSION

Two examples of the equiangular view of the rendered model of the room are shown as follows. Figure 7a displays the scene of the VNLS with distance between windows (d) = 0, interval of tilt angle (IA) = 2.0° , beam angle (BA) = 114° , total luminous flux (Φ) = 11100 lm; while Figure 7b displays the scene of real windows with $d = 0$, and average surface luminance (L_{av}) = 1800 cd/m^2 .

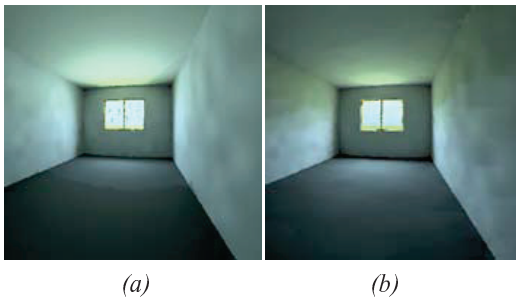


Figure 7 Impressions of the rendered view of the room with (a) VNLS with $d = 0$, IA = 2.0° , BA = 114° , $\Phi = 11100 \text{ lm}$; and (b) real window with $d = 0.75 \text{ m}$, $L_{av} = 1800 \text{ cd/m}^2$

Sensitivity analysis

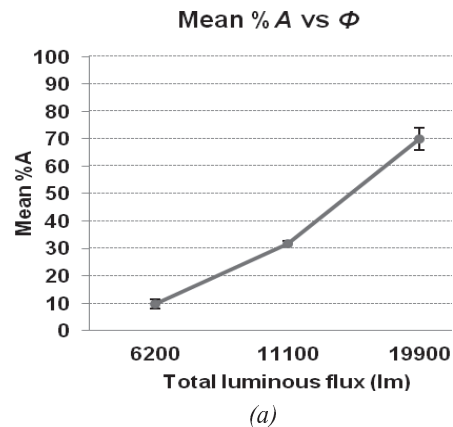
Table 2 displays the standard regression coefficient (β' [-]) of all input variables, i.e., the distance between windows (d), interval of tilt angle (IA), beam angle (BA), and total luminous flux (Φ); evaluated for the four performance indicators, i.e. the space availability (%A), uniformity (U_0), average ground contribution (% G_{av}), and average probability of discomfort glare (PDG $_{av}$) at position C.

Table 2 Standard regression coefficient of all input variables, i.e. d , IA, BA, and Φ ; evaluated for all performance indicators, i.e. %A, U_0 , % G_{av} , and PDG $_{av}$ at position C

Input \ Output	d	IA	BA	Φ
%A	-0.01	0.00	-0.13	0.98
U_0	0.12	-0.23	0.94	0.00
% G_{av}	-0.06	0.36	-0.82	-0.01
PDG $_{av}$	0.04	-0.09	-0.85	0.47

As shown, total luminous flux is the most influential input variable to space availability ($\beta' = 0.98$), while beam angle is found to be the most influential input variable to the other output variables ($\beta' = 0.94$ for U_0 , -0.82 for % G_{av} , and -0.85 for PDG $_{av}$). The output variables are then classified according to the most influential input variables. The relationship between the arithmetic mean of the output and the most influential input are illustrated in Figure 8, with the error bars indicating 95% confidence level.

The results show that the space availability is positively influenced by the total luminous flux. The output values increase with a factor of 3.2 when increased from 6200 lm to 11100 lm, and 2.2 when increased from 11000 lm to 19900 lm. Note that the total luminous flux values follow a logarithmic scale with an increment factor of around 1.8.



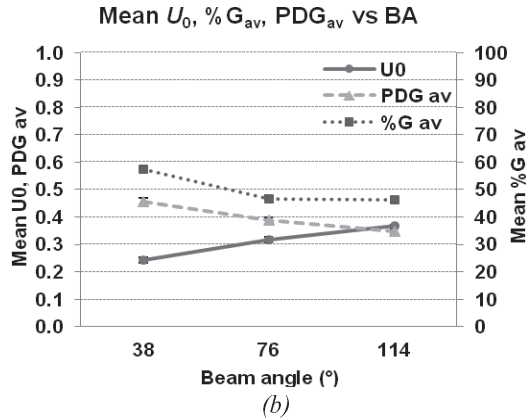


Figure 8 Graphs showing the relationship between the arithmetic mean of the output variables and the most influential input variables, i.e. (a) the space availability and (b) the beam angle. The error bars indicate 95% confidence level.

The uniformity, average ground contribution on the ceiling, and average probability of discomfort glare are highly influenced by the “sky” beam angle. The relationship between these input and output variables is almost perfectly linear, except for the average ground contribution, which values are decreased by around 10% (absolute difference), when the input is increased from 38° to 76°; but are only decreased by around 0.4% when the input is increased from 76° to 114°.

Comparison with real windows

Table 3 gives selected values of the ratio of space availability (%A), uniformity (U_0), and average ground contribution (% G_{av}) of each VNLS configuration to those of real windows having the same average surface luminance. It also displays the ratio of the average probability of discomfort glare (PDG_{av}) at position C in the real windows scene to that in a VNLS scene with the same average surface luminance. Note that only the configurations with total luminous flux of 11100 lm are shown in the table. The bold-typed values are those that satisfy the given criterion.

Most of the VNLS satisfying all criteria are those having a beam angle of 114° (wide spread). Most of the VNLS with beam angles of 38° (narrow spread) and 76° (medium spread) fail to create larger space availability relative to the real windows. The luminous intensity from a VNLS with a 114° beam angle is more evenly distributed throughout the space; therefore, more points on the workplane can reach the minimum illuminance of 500 lx. The appearance of the CIE overcast sky model for the real windows, which is typically characterised by an almost diffuse luminous intensity distribution pattern over the workplane, can be best approached by using a wide spread beam angle for the VNLS model. The

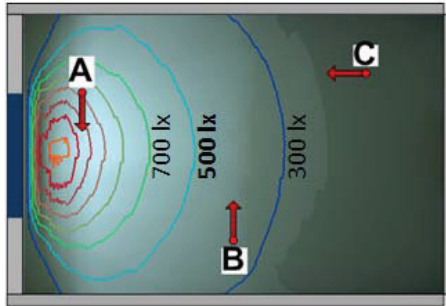
results are however limited to this specific sky model, and therefore nothing can be said yet about other sky conditions.

Table 3 Summary of the ratio of %A, U_0 , and % G_{av} of each VNLS configuration to those of real windows with the same average surface luminance; and the ratio of PDG_{av} at position C in the real windows scene to that in a VNLS scene with the same average surface luminance

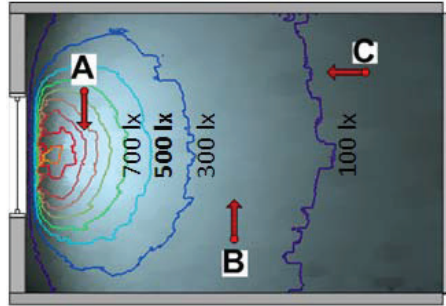
d [m]	IA [°]	BA [°]	Ratio %A	Ratio U_0	Ratio % G_{av}	Ratio PDG _{av}
0	1.0	38	0.5	1.4	1.1	0.9
0	1.5	38	0.5	1.2	1.1	0.9
0	2.0	38	0.5	1.1	1.2	1.0
0	1.0	76	1.2	2.0	0.9	0.9
0	1.5	76	1.2	1.8	0.9	0.9
0	2.0	76	1.1	1.7	1.0	0.9
0	1.0	114	2.1	2.1	0.9	1.0
0	1.5	114	2.0	2.1	0.9	1.0
0	2.0	114	2.0	2.1	1.0	1.0
0.75	1.0	38	0.5	1.6	1.1	0.9
0.75	1.5	38	0.6	1.4	1.2	0.9
0.75	2.0	38	0.6	1.3	1.2	1.0
0.75	1.0	76	1.1	2.3	0.9	0.9
0.75	1.5	76	1.1	2.1	0.9	0.9
0.75	2.0	76	1.1	2.1	1.0	1.0
0.75	1.0	114	2.1	2.3	0.9	1.0
0.75	1.5	114	2.1	2.3	1.0	1.0
0.75	2.0	114	2.0	2.2	1.0	1.0

Within the variations that satisfy all criteria, the ratio between space availability under VNLS and real windows scene is found to be 1.1 ~ 2.3; while for uniformity, the figure is between 1.4 ~ 2.5. For illustration, in an office of 19.4 m² floor areas as in this case, the real windows with an average surface luminance of 1800 cd/m² produce a daylit area of approximately 2.9 m². If VNLS of the same configuration with 114° beam angle and the same average surface luminance are used instead of the real windows, they produce a daylit area of approximately 5.7 m² ~ 6.0 m², which is a 100% increase. The uniformity is also increased from 0.16 in the real windows scene to 0.36 in VNLS scene.

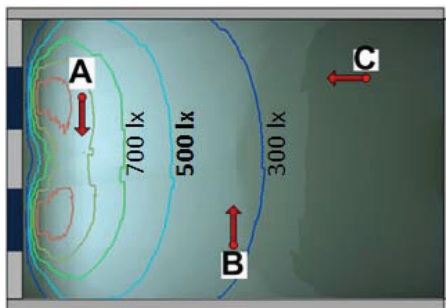
Figure 9 displays examples of isolux contour lines on the workplane of the VNLS configurations that satisfy all criteria, compared to the corresponding real windows configurations:



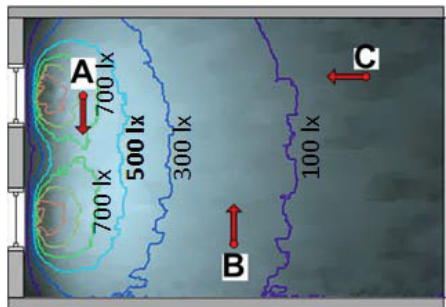
(a)



(b)



(c)



(d)

Figure 9 Isolux contour lines on the workplane of configurations (a) VNLS with $d = 0$, $IA = 2.0^\circ$, $BA = 114^\circ$, $\Phi = 11100$ lm; (b) real window with $d = 0$, $L_{av} = 1800$ cd/m²; (c) VNLS with $d = 0.75$ m, $IA = 2.0^\circ$, $BA = 114^\circ$, $\Phi = 11100$ lm; (d) real window with $d = 0.75$ m, $L_{av} = 1800$ cd/m²

- VNLS: $d = 0$, $IA = 2.0^\circ$, $BA = 114^\circ$, $\Phi = 11100$ lm, $L_{av} = 1800$ cd/m²
- Real window: $d = 0$, $L_{av} = 1800$ cd/m²

- VNLS: $d = 0.75$ m, $IA = 2.0^\circ$, $BA = 114^\circ$, $\Phi = 11100$ lm, $L_{av} = 1800$ cd/m²

- Real window: $d = 0.75$ m, $L_{av} = 1800$ cd/m²

The shown figures illustrate that the VNLS has a similar isolux pattern compared to the corresponding real windows. However, the contour lines for 500 lx values are located at different distances from the window. The area covered by the 500 lx contour line, which determines the space availability, in the VNLS scene is approximately double the size of that in the real windows one. Consequently, the uniformity under the VNLS is also larger compared to the real window, by approximately the same factor of two.

CONCLUSIONS AND OUTLOOK

The development of VNLS models with a simplified view using a lighting simulation tool has been demonstrated in this study. It shows the possibility to model the direction of light from the “ground” to the ceiling and from the “sky” to the floor. Based on the sensitivity analysis, it is concluded that:

1. The total luminous flux of VNLS positively influences the space availability.
2. The beam angle of VNLS positively influences the uniformity, and negatively influences average ground contribution on the ceiling and average probability of discomfort glare.
3. Most of the VNLS satisfying all criteria are those with a beam angle of 114° .

The VNLS models produce approximately 1.4 ~ 2.5 times larger space availability, compared to real windows under the CIE overcast sky. In this example of an office with 19.4 m² floor area, real windows with an average surface luminance of 1800 cd/m² produce a daylit area of approximately 2.9 m². On the other hand, VNLS with the same window configuration of 114° beam angle and the same average surface luminance can produce a daylit area of 5.7 m² ~ 6.0 m² in the same space. This shows the potential high performance of VNLS relative to real windows for the performance indicators tested.

The application of these new solutions can be further extended in larger (open-plan) offices, healthcare facilities, and industrial halls. The detailed settings largely depend on the building’s function. For example, in an industrial hall where the ceiling is relatively high, VNLS can be placed near the ceiling in a continuous row, to give more adequate light, without the needs of very detailed views. Meanwhile, in an ICU patient’s room, VNLS with a more complex view is presumably preferred, and the light output could be adjustable to follow the daily rhythm.

In term of impact on energy consumption, the detailed calculations are ongoing. Some simple calculations have been performed earlier, to predict the annual heating and cooling energy demand in reference rooms with and without VNLS (Mangkuto

et al., 2012b). The room with VNLS has a higher cooling energy demand than that with real windows, but it has significantly lower heating energy demand. The calculation was however based on a static operating schedule and the use of fluorescent lamps; should the schedule become dynamic and use a more energy-efficient light source, the predicted annual energy consumption will be even lower.

In addition, first verification of lighting measurement and simulation results in those reference rooms are also discussed in that particular paper.

It should be noticed that the described work in this paper reports only a part of the VNLS development, based on computational simulation tools. Additional studies involving more detailed image scenes, different sky conditions, as well as more features of real daylight that influence visual comfort, are required to improve the degree of similarity to real windows. Moreover, further subjective evaluation with users is also required to understand how people will actually appraise VNLS in reality.

Despite the limitation, the results of this study show clear examples on how building performance simulation contributes in the process of steering innovations, by demonstrating that the simulated model of some VNLS configurations has a better lighting performance than real windows.

NOMENCLATURE

$%A$	= space availability
$%G$	= ground contribution on the ceiling
$%G_{av}$	= average ground contribution on the ceiling
BA	= beam angle of the “sky” element
CGI_n	= normalised CIE glare index
d	= distance between individual windows
DGI_n	= normalised daylight glare index
DGP	= daylight glare probability
E_{av}	= average illuminance
E_{ground}	= illuminance contribution from the “ground” element on the ceiling
E_{min}	= minimum illuminance
E_{total}	= total illuminance on the ceiling
IA	= interval of tilt angle of the “sky” element
L_{av}	= average surface luminance of the window
N	= total number of points
$n(E \geq 500 \text{ lx})$	= percentage of the number of points with illuminance $\geq 500 \text{ lx}$
PDG_{av}	= average probability of discomfort glare
U_0	= uniformity
UGR_n	= normalised unified glare rating
β'	= standard regression coefficient
Φ	= total luminous flux of the “sky” element

ACKNOWLEDGEMENT

This work is supported by the Sound Lighting research line of the Intelligent Lighting Institute, Eindhoven University of Technology.

REFERENCES

- Boyce, P.R., Hunter, C., Howlett, O. 2003. *The Benefits of Daylight Through Windows*. Troy, New York: Lighting Research Center.
- CEN. 2002. "EN 12464-1: Light and Lighting - Lighting of work places, Part 1: Indoor work places." Brussels: Comité Européen de Normalisation.
- Diepens, J.F.L., Bakker, F., Zonneveldt, L. 2000. *Daylight Design Variations Book*. TNO-TUE Centre for Building Research. Retrieved 14 August 2012, from <http://sts.bwk.tue.nl/daylight/varbook/index.htm>
- Heschong, L. 2003. *Window and Offices: A Study of Office Worker Performance and the Indoor Environment*. P500-03-082-A-9. Gold River, CA: Heschong Mahone Group.
- Heschong, L., Wright, R.L., Okura, S. 2002. Daylighting impacts on human performance in school. *Journal of the Illuminating Engineering Society*, 31(2), 101-114.
- Jakubiec, J.A., Reinhart, C.F. 2012. The 'adaptive zone' – A concept for assessing discomfort glare throughout daylight spaces. *Lighting Research and Technology*, 44(2), 149-170.
- Lawrence Berkeley National Laboratory (LBL). *Virtual Lighting Simulator*. 2010. Retrieved 14 August 2012, from <http://gaia.lbl.gov/vls/>.
- Mangkuto, R.A., Aries, M.B.C., Loenen, E.J. van, Hensen, J.L.M. 2011. Properties and performance indicators of virtual natural lighting solutions. *Proceedings of CISBAT 2011*, 14-16 September 2011, pp. 379-384. Lausanne: École Polytechnique Fédérale de Lausanne.
- Mangkuto, R.A., Aries, M.B.C., Loenen, E.J. van, Hensen, J.L.M. 2012a. Lighting performance of virtual natural lighting solutions with a simplified image in a reference office space. *Proceedings of Experiencing Light 2012*, 12-13 November 2012, pp. 1-5. Eindhoven: Eindhoven University of Technology.
- Mangkuto, R.A., Ochoa, C.E., Aries, M.B.C., Loenen, E.J. van, Hensen, J.L.M. 2012b. Simulaties voor R&D: 'Virtual Natural Lighting' systemen. *TVVL Magazine*, 5(2012), 38-40. [in Dutch: Simulations for R&D: 'Virtual Natural Lighting' systems]
- Shin, J.Y., Yun, G.Y., Kim, J.T. 2012. View types and luminance effects on discomfort glare assessment from windows. *Energy and Buildings*, 46(2012), 139-145.
- Tregenza, P.R. 1989. Modification of the split-flux formulae for mean daylight factor and internal reflected component with large external obstructions. *Lighting Research and Technology*, 21(3), 125-128.
- Wienold, J., Christoffersen, J. 2006. Evaluation methods and development of a new glare prediction model for daylight environments with the use of CCD cameras. *Energy and Buildings*, 38(2006), 743-757.
- van Dijk, D., Platzer, W.J. 2003. Reference office for thermal, solar and lighting calculations. *Report no. swift-wp3-tno-dvd-030416*.